Available online at www.sciencedirect.com
ScienceDirect
Journal of the European Ceramic Society 31 (2011) 629–635
www.elsevier.com/locate/jeurceramsoc

Influence of β-Si_3N_4 particle size and heat treatment on microstructural evolution of α:β-SiAlON ceramics

N. Calis Acikbas [a,*], R. Kumar [b], F. Kara [c], H. Mandal [c], B. Basu [b]

[a] *MDA Advanced Ceramics, Ltd. Co., Eskisehir, Turkey*
[b] *Laboratory for Advanced Ceramics, Department of Materials and Metallurgical Engineering, Indian Institute of Technology, IIT, Kanpur, India*
[c] *Anadolu University, Department of Materials Science and Engineering, Eskisehir, Turkey*

Received 23 June 2010; received in revised form 27 September 2010; accepted 3 October 2010
Available online 18 November 2010

Abstract

In the present study, we report the effects of starting β-Si_3N_4 particle sizes and post-sintering heat treatment on microstructure evolution and mechanical properties of prepared α–β SiAlON ceramics. Three different β-Si_3N_4 starting powders, with particle sizes of 2, 1 and 0.5 μm were used to prepare α–β SiAlON ceramics by gas-pressure sintering. Elongated β-SiAlON grain morphology was identified in the samples prepared using 0.5 μm particle size β-Si_3N_4 powder. Low-aspect ratio grain morphology was observed in samples prepared from starting powders with coarse particles (2 μm and 1 μm). The sintered samples were further heat treated to develop desired microstructure with elongated grains. The hardness and indentation fracture toughness values of sintered and heat treated samples were found to lie in the range of 12.4–14.2 GPa and 5.1–6.4 MPa $m^{1/2}$ respectively. It was revealed that fracture toughness increases with decrease in particle size of starting β-Si_3N_4 powder.

Keywords: Sialon; Milling; Sintering; Hardness; Microstructure-final

1. Introduction

Among various engineering ceramics, silicon nitride (Si_3N_4) based ceramics are widely researched because of their low density, high hardness, toughness and wear resistance.[1–5] It has been widely recognized that mechanical properties of these ceramics such as hardness and fracture toughness are strongly dependent on the grain morphology. SiAlONs are a class of silicon nitride ceramics. There are two SiAlON phases that are of interest as engineering ceramics: α and β. While β-SiAlON has higher toughness, strength and thermal conductivity, α-SiAlON has higher hardness but usually lower strength and toughness values. α- and β-SiAlON phases are completely compatible and they are readily prepared by a single stage sintering of the appropriate mixtures of nitrides and oxides leads to the formation of α- and β-SiAlON phases.[6] Complete compatibility of α- and β-SiAlON phases, easier fabrication and higher chemical resistance compared to Si_3N_4 ceramics has resulted in more attention towards mixed α:β SiAlON ceramics. Also, it is important to mention that the resulting mixed composition has good mechanical properties due to the combination of high hardness of α-SiAlON and good strength and toughness of β-SiAlON.[7]

Microstructural evolution of SiAlON ceramics is controlled by the properties of starting Si_3N_4 powder, sintering additives and processing conditions. Generally, two forms of silicon nitride exist as starting powder: α-Si_3N_4 and β-Si_3N_4. Wild et al.[8] have shown that a small amount of oxygen is incorporated into the atomic structure of the α phase with the approximate formula as $Si_{11.5}N_{15}O_{0.5}$; whereas the β-phase is pure β-Si_3N_4. Typically, α-Si_3N_4 has higher reactivity and is used more commonly than β-Si_3N_4. Other reason for the preference of α-Si_3N_4 powder is easy attainment of elongated β-Si_3N_4 grain morphology after α → β phase transformation during sintering.[9] α-Si_3N_4 phase is a low temperature configuration and transforms to β-phase around 1410 °C.[10] On the other hand, when β-Si_3N_4 powder is used as starting powder, elongated grain formation and densification are rather difficult.[11] The types of sintering additive and sintering conditions are also important for microstructural

* Corresponding author. Present address: Department of Mechanical and Manufacturing Engineering, Bilecik University, Bilecik, Turkey.
Tel.: +90 222 2361880; fax: +90 222 2361881.
E-mail addresses: nurcan.acikbas@bilecik.edu.tr, ncalis@gmail.com, ncalis@anadolu.edu.tr (N.C. Acikbas).

0955-2219/$ – see front matter © 2010 Elsevier Ltd. All rights reserved.
doi:10.1016/j.jeurceramsoc.2010.10.001

evolution. Most of the research has been focused on the influence of sintering additives on grain growth.[12,13] Gas-pressure sintering of Si_3N_4 ceramics at higher temperatures (>1800 °C) results in in situ composite microstructures with high fracture toughness.[14] Another way to obtain elongated grain morphology is to heat treat the sintered sample at high temperatures.[14–17]

There exist some studies on microstructural evolution of SiAlON ceramics using different β-Si_3N_4 starting powders.[18–21] Ekström et al.[18] used five different Si_3N_4 powders, containing up to 15% β-Si_3N_4. High content of β-Si_3N_4 phase in the starting powder resulted in higher β:α SiAlON ratio in the sintered material. This observation was explained by the fact that nucleation and growth of a β-SiAlON grain may start from the β-Si_3N_4 seeds present as undissolved crystallites. However, no substantial difference was observed in the microstructural development of the five starting powders, probably due to already high α-Si_3N_4 content of the starting powders. In another study, Li et al.[19] used three different Si_3N_4 starting powders with similar particle size, but different α:β phase ratios (100α, 50α:50β and 100β). The aim of the study was to investigate the effect of α:β phase ratio on densification behavior, phase assembly and microstructural development of Ca-α-SiAlON ceramics. Poorer densification was observed for powders with β-Si_3N_4 due to low reactivity. However, the final phase assembly of Ca α-SiAlON composition was not affected significantly by the different Si_3N_4 starting powders used. Low-aspect ratio grain evolution was observed in the samples with higher β phase starting powder. The reason for this was attributed to lower solubility of β-Si_3N_4 powder causing high viscosity and low liquid content during sintering. Also, heterogeneous nucleation was thought to be a possible mechanism for α-SiAlON grain evolution due to much higher Gibbs free energy required in the formation of nuclei for homogeneous nucleation, when β-Si_3N_4 powder was used. Rosenflanz[20] observed that coarse β-Si_3N_4 powders (d_{50}: ~3 μm) delayed transformation to α-SiAlON. This provided a better chance for yielding lower nucleation rates, smaller nuclei density and forming of elongated α-SiAlON grains. On the other hand, when fine β-Si_3N_4 powder (d_{50}: ~1 μm) was used, an equiaxed microstructure was formed.

It was observed that studies on the use of pure β-Si_3N_4 powder are limited in reference to the development of α:β-SiAlON ceramics. Therefore, the aim of this study is to evaluate the effect of using different starting powder with varying particle sizes on the microstructure and phase development as well as to correlate these with the mechanical properties.

2. Experimental procedure

The starting β-Si_3N_4 powder (Beijing Chanlian-Dacheng Trade Co., Ltd., China) was produced by combustion synthesis and consisted 100% β-Si_3N_4 phase. Table 1 provides the chemical analysis (wt%) of as-received β-Si_3N_4 powder, which contains 3 wt% oxygen. Primary particle size of β-Si_3N_4 powder was measured to be around 4 μm. Attrition milling in water was performed to decrease the average particle size of β-Si_3N_4 starting powder to 2 μm, 1 μm and 0.5 μm. The corresponding starting powders were designated as B2 (d_{50}: 2 μm), B1 (d_{50}: 1 μm) and B05 (d_{50}: 0.5 μm). Table 2 lists the particle size distributions of the as-received and attrition milled (B2, B1 and B05) β-Si_3N_4 powders. Representative SEM images of as-received and milled β-Si_3N_4 powders are shown in Fig. 1. For comparative purpose, an α-Si_3N_4 powder with about 2.1 μm particle size (Grade S, HC-Starck) was also used (Table 2).

Table 1
Chemical analyses of as-received β-Si_3N_4 powder.

	Al_2O_3	MgO	CaO	Fe_2O_3	TiO_2	Sm_2O_3	Y_2O_3	Hf_2O_3
wt%	1.42	≤0.05	0.40	0.60	0.07	≤0.05	≤0.05	≤0.05

Table 2
Particle size distributions of the Si_3N_4 powders.

Starting powders	B (as-received)	B2	B1	B05	A (as-received)
d_{50} (μm)	10.0	2.1	1.2	0.5	2.1
d_{90} (μm)	36.0	4.8	2.4	1.4	4.5
d_{10} (μm)	2.4	0.7	0.5	0.2	0.7
Milling time (h)	–	4.0	9.0	21.0	–

To utilize the hardness of α-SiAlON and toughness of β-SiAlON, a composition of 30α:70β SiAlON was designed on the basis of our previous work.[21] Y–Sm–Ca multi-cation doping was chosen with an aim to produce self-reinforced microstructure. All of the designed SiAlON compositions starting with α- or β-Si_3N_4 powders were milled in water by using Si_3N_4 balls. The samples were uniaxially pressed at 25 MPa and subsequently cold isostatically pressed at 300 MPa to obtain uniform green density. The samples were then sintered by gas-pressure sintering route under 2.2 MPa nitrogen gas pressure at 1800 °C for 1 h and 1940 °C for 2 h depending on the initial particle size. The post-sintering heat treatment was performed at 1990 °C for 5 h under 2.2 MPa nitrogen gas pressure to facilitate grain growth. Archimedes principle was applied to measure the density of samples. The phase ratio, α:β-SiAlON, was determined by X-ray diffraction analyses (Rigaku Rint 200, Tokyo, Japan). Polished surfaces of the samples were gold coated prior to examination in a Zeiss VP50-Supra type scanning electron microscope (SEM) by using back-scattered electron imaging mode.

The mechanical properties, in particular hardness and indentation fracture toughness of the samples were determined by indenting the mirror polished surfaces by applying a load of 10 kg for 10 s using Vickers hardness tester. At least five indentations were made for each sample. The Vickers hardness (HV) was calculated using the following expression (Evans and Charles[22]):

$$HV_{10} = \frac{0.47P}{a^2} \quad \text{(i)}$$

where, HV_{10} is the Vickers hardness, P is load applied and a is half the length of the diagonal of the indentation produced by the indenter. The fracture toughness (K_{IC}) has been evaluated using the indentation fracture (IF) toughness technique. In the present work, the indentation fracture toughness K_{IC} (MPa $m^{1/2}$)

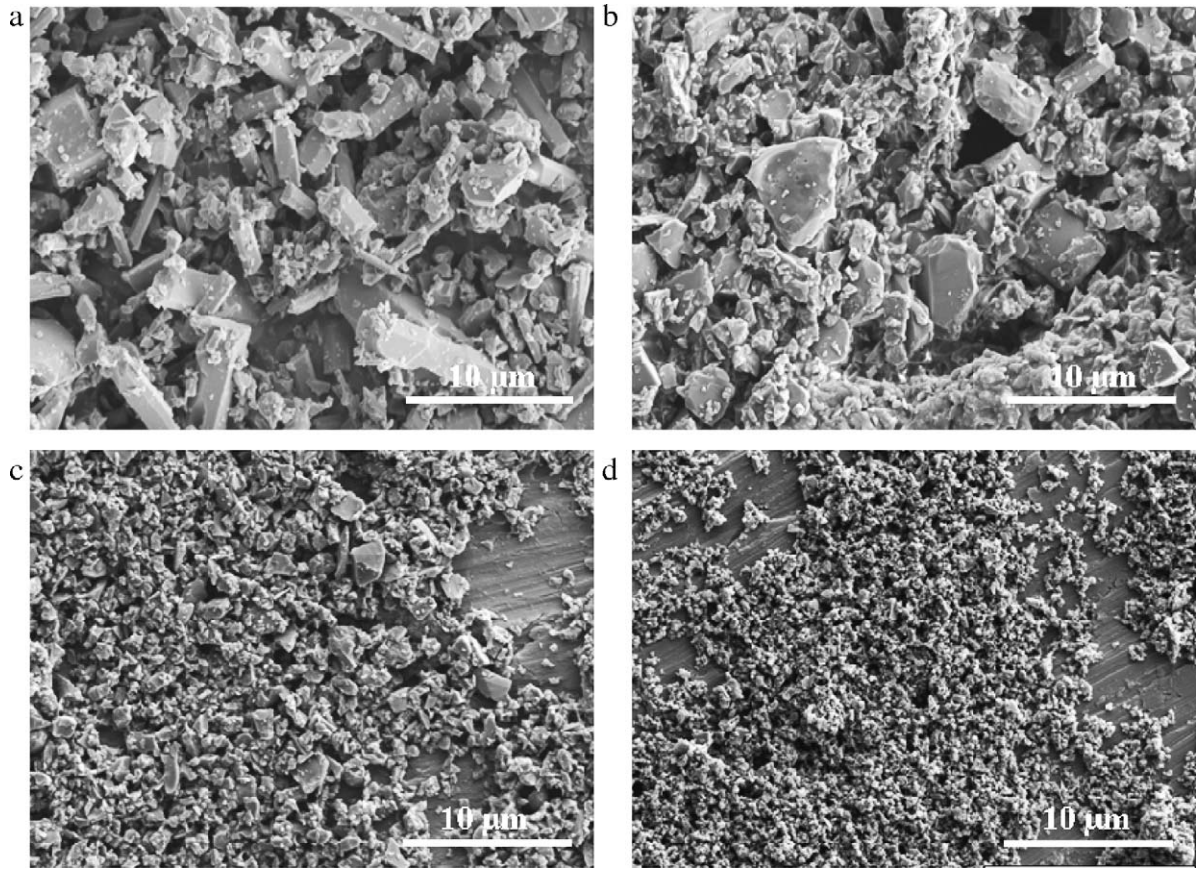

Fig. 1. Scanning electron microscope (SEM) image of (a) as-received β-Si_3N_4 powder, (b) B2, (c) B1 and (d) B05 powders.

has been calculated using the appropriate formula proposed by Niihara et al.[23] for median cracks:

$$K_{IC} = 0.018 \times H \times a^{0.5} \times \left(\frac{E}{H}\right)^{0.4} \times \left(\frac{(c-a)}{a}\right)^{-0.5} \quad \text{(ii)}$$

where $2a$ is the average indent diagonal length (μm), $2c$ is the crack length (from one crack tip to another), E is the elastic modulus (GPa) and H is the hardness (GPa). Both the indent diagonal and crack length were carefully measured from SEM images of the indented surfaces and the reported hardness and fracture toughness values are the average of at least five indentation measurements.

3. Results and discussion

3.1. Sintering and microstructural characterization

3.1.1. Effect of β-Si_3N_4 particle size

Sintering of the samples prepared from all three powders at 1940 °C for 2 h provided full densification. Sintering of B2 and B1 powders resulted in 30α:70β-SiAlON composition, while sintering of B0.5 powder gave rise to 100% β-SiAlON. This can be attributed to hydrolysis of β-Si_3N_4 powder during prolonged milling to 0.5 μm. It was verified by the measurement of the oxygen content of B0.5 which was measured to be 7.8 wt%. During milling in water following reaction of the Si_3N_4 powder can occur[24]:

$$Si_3N_4 + 6H_2O \rightarrow 3SiO_{2\,amorphous} + 4NH_3 \quad \text{(iii)}$$

SiO_2 formation due to this reaction shifts the composition to β-SiAlON rich region as shown in Fig. 2.[25] It is also expected that increased silica would preferentially react with α-SiAlON stabilizing additives and this would reduce/prevent α-SiAlON formation. It should also be mentioned that increased amount of liquid phase due to high oxygen content of B0.5 powder makes α → β-SiAlON transformation occur readily.[26] Higher oxygen

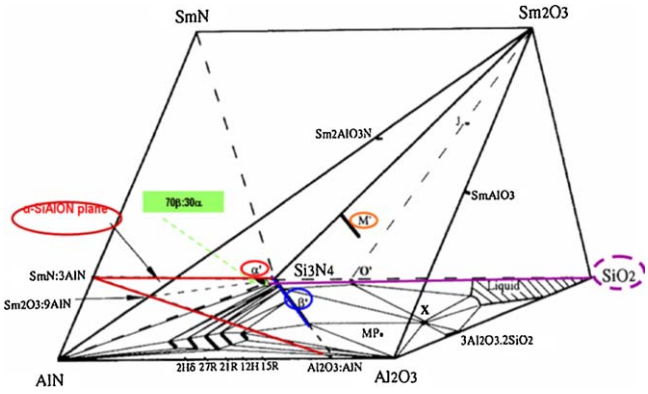

Fig. 2. Representation of Sm(Nd)–SiAlON system showing phases occurring in the region bound by Si_3N_4, $Sm(Nd)_2O_3$, Al_2O_3, and AlN, and SiAlON behavior diagram at 1700 °C.

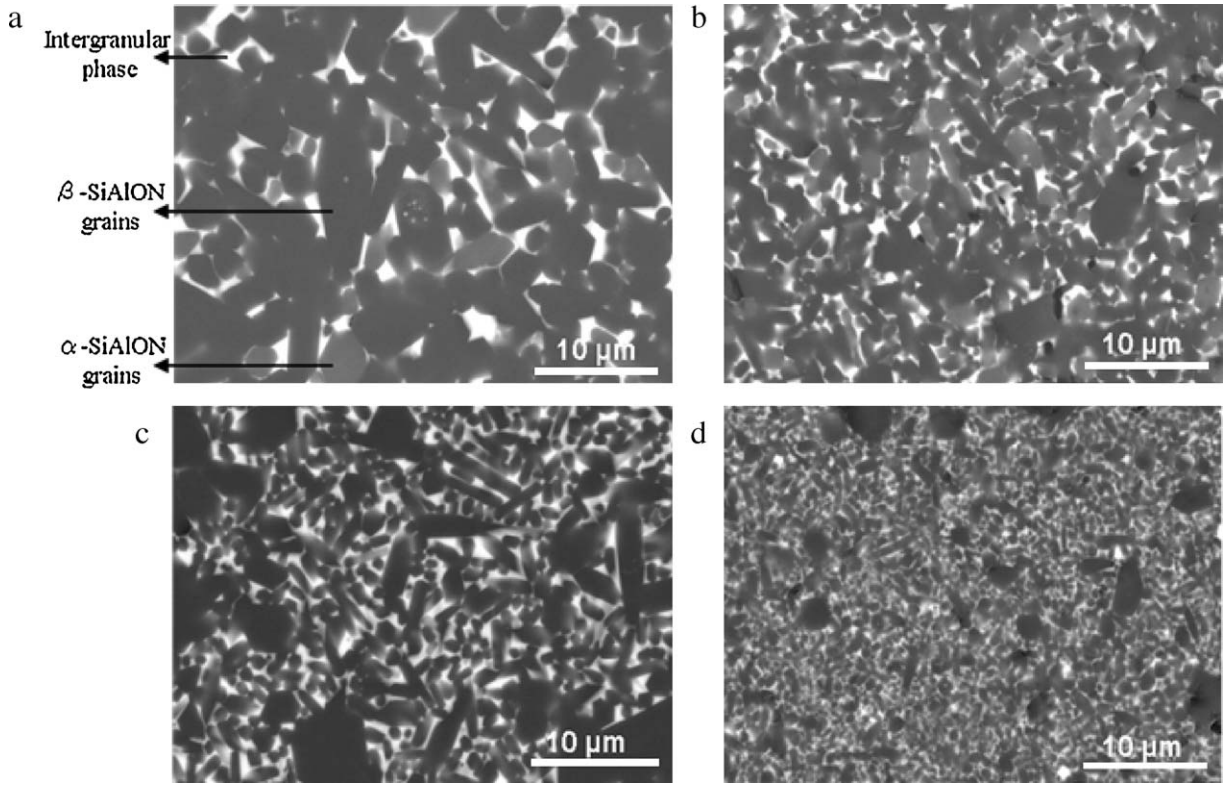

Fig. 3. BSE-SEM images representing the microstructure of samples (a) SB2 (b) SB1 and (c) B05 sintered at 1940 °C for 2 h (d) SB05 (dark grey grains are β-SiAlON, light grey grains are α-SiAlON and white areas are intergranular phase). The sample designations are mentioned in Table 3.

content results in more liquid phase during sintering and leads to better densification even at 1800 °C for B05 composition, although higher amount of liquid phase may degrade the high temperature properties.

Fig. 3 shows SEM micrographs of gas-pressure sintered SiAlONs prepared using three different Si_3N_4 starting powders (B2, B1 and B05) at 1940 °C and 1800 °C. It was observed that B05 can even be sintered at 1800 °C. The microstructure of SB2 (see Table 3 for nomenclature of samples) specimen consisted of predominantly 2–3 μm α- and β-SiAlON grains, mainly equiaxed in nature but some elongated grains with low-aspect ratio of 2–4 were also present (Fig. 3a). A decrease in β-Si_3N_4 particle size to 1 μm (B1) resulted in decrease in α- and β-SiAlON grain diameter to around 1 μm, but the aspect ratio of grains improved to about 2.5–7 (Fig. 3b). Subsequent reduction in initial powder particle size to 0.5 μm (B05) caused bimodal grain size distribution, when sintered at 1940 °C. Large grains with fairly high aspect ratio (7–8) were dispersed within a fine grain matrix of about 0.5 μm (Fig. 3c). However, sintering of B05 powder at 1800 °C for 1 h resulted in a fine grained equiaxed microstructure with grain size of 0.5 μm (Fig. 3d). Clearly, sintering at higher temperature facilitates the growth of elongated grain morphology (compare Fig. 3c and d). Therefore, it is evident that the grain size of β-Si_3N_4 derived SiAlON ceramics depend on the initial β-Si_3N_4 particle size. Fig. 4 shows the SEM micrograph of SiAlON (30α:70β) produced from α-Si_3N_4 powder with particle size of 2 μm. The micrograph consists of a bimodal microstructure with well developed elongated β-SiAlON grains and fine (∼1 μm) equiaxed grain matrix of primarily α-SiAlON, which is in contrast to SiAlON produced from β-Si_3N_4 powder (Fig. 3a).

During sintering, the solution of β-Si_3N_4 in the liquid phase and precipitation as α:β-SiAlON could have caused the formation of α:β-SiAlON from β-Si_3N_4 powder.[18] The nucleation can

Table 3
The detailed indentation data including, the crack length (*l*), indent diagonal length (2*a*) as well as the indentation toughness data for the gas pressure sintered SiAlON ceramics. HT stands for heat treatment conditions.

Sample	Sintering conditions	*l* (μm)	*a* (μm)	*l*/*a*
SB2	1940 °C, 2 h, 2.2 MPa N_2	97.8	57.2	1.7
SB1	1940 °C, 2 h, 2.2 MPa N_2	91.0	57.0	1.6
SB05	1800 °C, 1 h, 2.2 MPa N_2	80.2	59.5	1.3
HTB2	1940 °C, 2 h, 2.2 MPa N_2HT: 1990 °C, 5 h, 2.2 MPa N_2	87.8	58.4	1.5
HTB1	1940 °C, 2 h, 2.2 MPa N_2HT: 1990 °C, 5 h, 2.2 MPa N_2	82.9	56.1	1.5
HTB05	1800 °C, 1 h, 2.2 MPa N_2HT: 1990 °C, 5 h, 2.2 MPa N_2	61.6	60.9	1.0

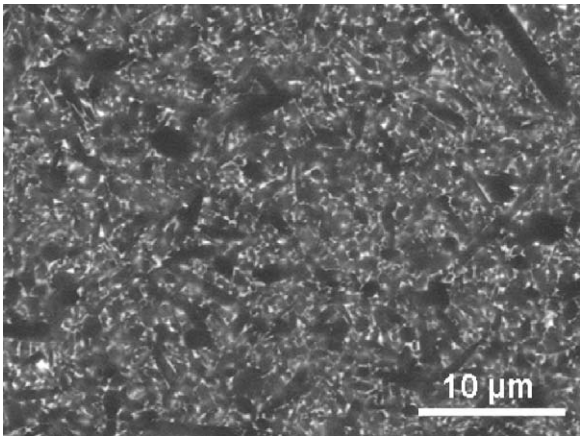

Fig. 4. Representative back-scattered SEM image of SiAlON prepared from coarse α-Si_3N_4 powder (average particle size is around 2 μm).

either be homogeneous from the liquid or heterogeneous on the existing β-Si_3N_4 grains. Given the fact that the use of coarse and fine β-Si_3N_4 powders results in coarse and fine α:β-SiAlON, respectively, it appears that nucleation of α:β-SiAlON occurs heterogeneously on the preexisting crystals in case of B2 and B1 powders. In contrast, when 2 μm α-Si_3N_4 powder is used, the grain size of SiAlON is 1 μm or less. This indicates their α-SiAlON powder dissolves and precipitates SiAlON by homogeneous nucleation. Aspect ratio of α-SiAlON grains was found to be similar with β-SiAlON grains in SB1 and SB2 samples.

Previous studies[18,27] indicate that nucleation and growth of a β-SiAlON grain generally proceed from β-Si_3N_4 seeds. Rosenflanz[20] studied sintering of α-SiAlON ceramics using β-Si_3N_4 powder with 1 and 3 μm average particle sizes. He observed that when 1 μm β-Si_3N_4 powder was used, an equiaxed α-SiAlON microstructure developed, whereas when 3 μm β-Si_3N_4 powder was used, some of the α-SiAlON grains were elongated, in contrast to the present study. The difference may be due to the fact that Rosenflanz studied with pure α-SiAlON system.

Since the solubility rate of coarse B2 powder is expected to be less than finer B1 powder, liquid phase will have a low viscosity in case of B2 powder due to its lower nitrogen and silicon content. Low viscosity of liquid phase leads to fast reduction of the supersaturation and a lower final aspect ratio. The aspect ratio of grains during precipitation depends primarily on the viscosity of the liquid phase and the diffusion rate, high viscosity of the liquid phase leads to a slow reduction of supersaturation and a higher final aspect ratio.[27] Apart from viscosity, grain size is a critical factor for grain growth. Smaller grains have smaller radius of curvature and more driving energy to move, change shape and even to be consumed by larger grains.[28] B2 and B1 powders resulted in 2 and 1 μm average grain size with relatively equiaxed shape and straight interfaces. On the contrary,

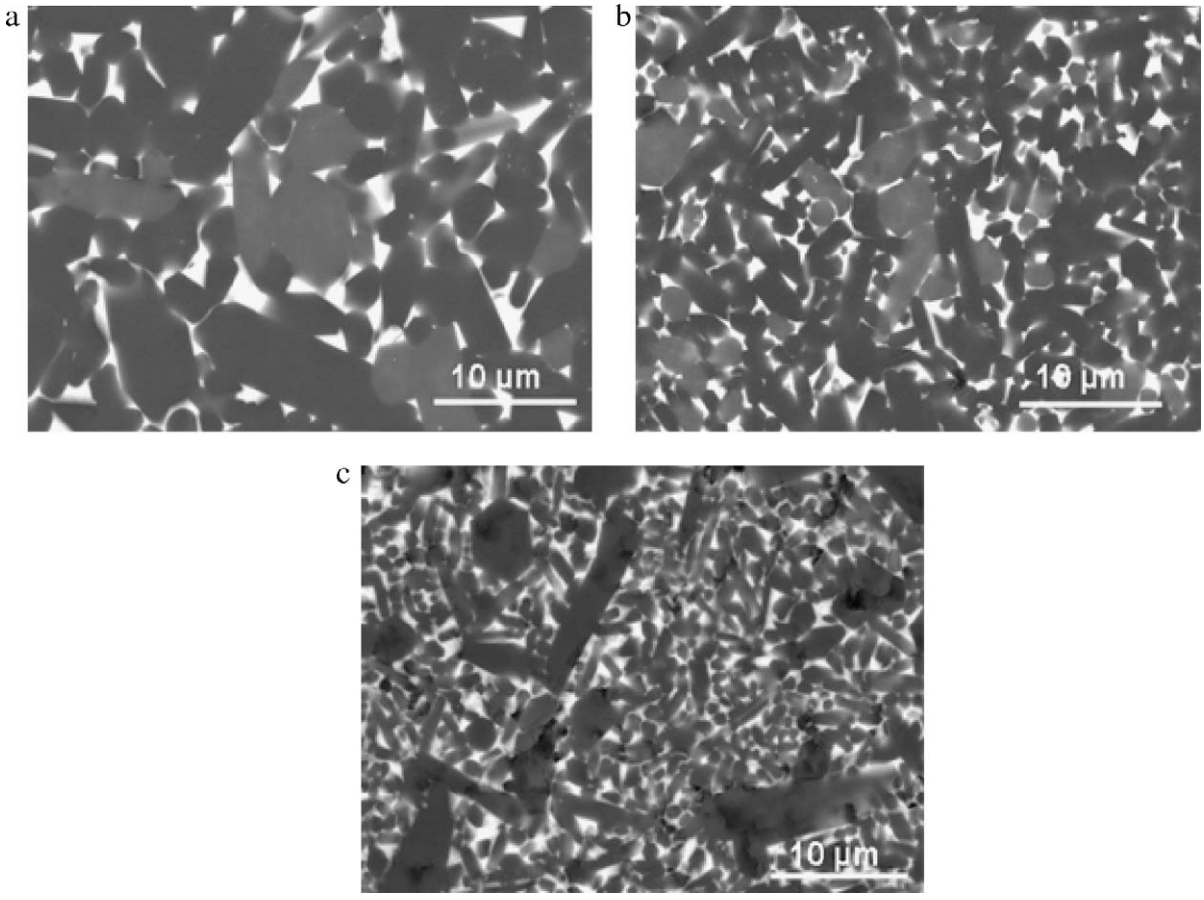

Fig. 5. BSE-SEM images representing the heat treated microstructure of samples (a) HTB2 (b) HTB1 and (c) HTB05. The sample designations are mentioned in Table 3.

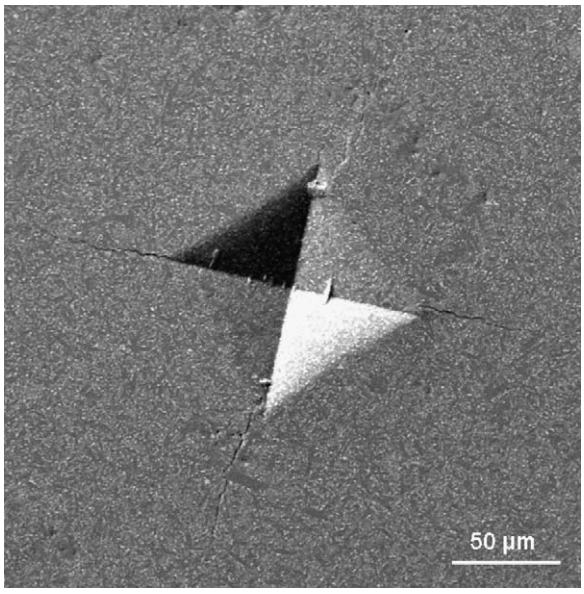

Fig. 6. SEM topography image of the Vickers indent and indentation-induced radial crack pattern of SB1 sample.

B0.5 powder resulted in finer grain size and irregular interfaces providing high driving force for grain growth. In turn, abnormal grain growth took place and left behind a bimodal grain size distribution.

3.1.2. Effect of heat treatment

When heat treatment at 1990 °C for 5 h was applied to the SiAlONs produced from different starting powders, no marked difference was observed in the microstructures of SiAlONs produced from B2 and B1 (see Figs. 3a and 5a and Figs. 3b and 5b) except increase in β-SiAlON content up to 90% and 80% respectively. The reason for increased amount of β-SiAlON with heat treatment is due to the fact that during heat treatment, α-SiAlON stabilizing cations go into liquid phase, causing transformation from α- to β-SiAlON. In addition, increased amount of liquid phase increases tendency of α- to β-SiAlON transformation.[26,29] However, substantial grain growth was observed in HTB05 SiAlON, giving desired microstructures of large elongated grains distributed in a fine grained matrix (see Figs. 3d and 5c). It is evident that in order to achieve grain growth and to develop self-reinforced microstructure after heat treatment, the grain size of SiAlON after sintering should be rather fine, preferably less than 0.5 μm as in Fig. 3d. Otherwise, coarse grains, even around 1 μm, do not have enough driving force for grain growth. Similar observations were made by others on β-Si_3N_4 ceramics.[14–17] Lee et al.[15] showed that sintering of β-Si_3N_4 ceramics (prepared from β-Si_3N_4 of 0.66 μm in average size) at 1850 °C results in equiaxed β-Si_3N_4 grains. An increase in sintering temperature to 2000 °C causes the development of elongated grains.

3.2. Mechanical properties

Fracture toughness of the SiAlONs was measured by Vickers indentation technique. The Vickers indents were analyzed by SEM in order to study the indentation cracking behavior. Fig. 6 shows a typical Vickers indent and indentation-induced radial crack pattern in the SiAlON ceramic. Both indent diagonals and crack lengths around the indentations were measured from the SEM images and are given in Table 3. The hardness and fracture toughness of the studied ceramics are summarized in Table 4. From Table 3, it is clear that *l*/*a* ratio varies between 1.0 and 1.7 and such values indicate good crack growth resistance property of the investigated ceramics. On the basis of observations made from Figs. 3 and 5 and Table 4, the microstructure–property correlation can be discussed. The differences in microstructure and properties can be explained on the basis of differences in powder particle size as well as due to the combination of sintering and heat treatment conditions. The reduction in hardness values after heat treatment can be correlated with the growth of equiaxed grains and change in phase assemblage where α-SiAlON content decreases with heat treatment (Table 4). The difference in hardness between SB2, SB1 with that of SB05 can be ascribed to the presence of larger fraction of grain boundary phase in SB05 due to prolonged milling and also to the absence of harder α-SiAlON phase. However, the development of more elongated grains in SB05 results in relatively higher toughness than other sintered ceramics. On similar account, high toughness is also measured in case of HTB05 ceramic, compared to that of HTB2 and HTB1 ceramics. In particular, well developed elongated grains in HTB05 can lead to more effective crack bridging and deflection.

Table 4
Mechanical properties and developed phases of SiAlONs, prepared with different initial particle sizes 2 μm (B2), 1 μm (B1) and 0.5 μm (B05), when subjected to sintering and then heat treatment.

Sample	HV (GPa)	K_{IC} (MPa $m^{1/2}$)	Phases
SB2	14.1 ± 0.04	5.1 ± 0.16	78β:22α
SB1	14.2 ± 0.03	5.3 ± 0.02	73β:27α
SB05	13.0 ± 0.03	5.6 ± 0.20	100β
HTB2	13.5 ± 0.05	5.4 ± 0.18	90β:10α
HTB1	13.6 ± 0.01	5.6 ± 0.14	80β:20α
HTB05	12.4 ± 0.01	6.4 ± 0.41	100β

4. Conclusions

In the present study, the effects of starting β-Si_3N_4 particle sizes and post-sintering heat treatment on microstructure evolution and mechanical properties have been investigated. It was observed that marked differences in microstructures can be obtained by starting with different particle sizes of β-Si_3N_4 powders. Initial particle size is of primary importance to achieve bimodal microstructure and hence, improved fracture toughness. The development of α:β-SiAlONs with self-reinforced microstructure and elongated grains requires the use of fine (≤0.5 μm) β-Si_3N_4 starting powder. However, even coarse α-Si_3N_4 (2 μm) gives fine and elongated microstructure. A good combination of hardness of around 12 GPa and indentation toughness of 6.4 MPa $m^{1/2}$ can be obtained in ceramics sintered from finest (≤0.5 μm) β-Si_3N_4 powders.

References

1. Kumar R, Acikbas NC, Kara F, Mandal H, Basu B. Microstructure–mechanical properties–wear resistance relationship of SiAlON ceramics. *Metall Mater Trans A* 2009;**40**:2319–32.
2. Basu B, Manisha, Mukhopadhyay NK. Understanding the mechanical properties of hot pressed Ba-doped S-Phase SiAlON ceramics. *J Eur Ceram Soc* 2009;**29**:801–11.
3. Manisha, Basu B. Tribological properties of a hot pressed Ba-doped S-phase sialon ceramic. *J Am Ceram Soc* 2007;**90**:1858–65.
4. Basu B, Lewis M, Smith ME, Bunyard M, Kemp T. Microstructure development and properties of novel Ba-doped S-phase sialon ceramics. *J Eur Ceram Soc* 2006;**26**:3919–24.
5. Basu B, Vleugels J, Kalin M, Van Der Biest O. Friction and wear mechanism of sialon ceramics under fretting contacts. *Mater Sci Eng A* 2003;**359**:228–36.
6. Riley FL. Silicon nitride and related materials. *J Am Ceram Soc* 2000;**83**:245–65.
7. Jack KH, Wilson WI. Ceramics based on the Si–Al–ON and related systems. *Nat (London) Phys Sci* 1972;**238**:28–9.
8. Wild S, Grieveson P, Jack KH, Popper P. *Special ceramics 5*. The British Ceramic Research Association; 1972.
9. Lee DD, Kang SJL, Petzow G, Koon DK. Effect of α to β (β′) phase transition on the sintering of silicon nitride ceramics. *J Am Ceram Soc* 1990;**73**:767–9.
10. Mandal H, Thompson DP, Ekström T. Reversible α sialon transformation in heat-treated sialon ceramics. *J Eur Ceram Soc* 1993;**12**: 421–9.
11. Lee SK, Lee KS, Lawn BR, Kim DK. Effect of starting powder on damage resistance of silicon nitrides. *J Am Ceram Soc* 1998;**81**:2061–70.
12. Hampshire S, Jack KH. In: Riley FL, editor. *Progress in nitrogen ceramics*. Boston: Martinus Nijhoff Publishers; 1983. p. 225–30.
13. Ziegler G, Heinrich J, Wotting G. Relationships between processing, microstructure and properties of dense and reaction-bonded silicon nitride. *J Mater Sci* 1987;**22**:3041–86.
14. Mitomo M, Tsutsumi H, Tanaka S, Uenosono S, Saito F. Grain growth during gas-pressure sintering of β-silicon nitride. *J Am Ceram Soc* 1990;**73**:2441–5.
15. Lee CJ, Chae JI, Kim DJ. Effect of [beta]-Si_3N_4 starting powder size on elongated grain growth in [beta]-Si_3N_4 ceramics. *J Eur Ceram Soc* 2000;**20**:2667–71.
16. Mitomo M, Hirotsuru H, Suematsu H, Nishimura T. Fine-grained silicon nitride ceramics prepared from β-powder. *J Am Ceram Soc* 1995;**78**:211–4.
17. Hirosaki N, Akimune Y, Mitomo M. Effect of grain growth of β-silicon nitride on strength, Weibull modulus, and fracture toughness. *J Am Ceram Soc* 1993;**76**:1892–4.
18. Ekström T, Ingelström N, Brage R, Hatcher M, Johansson T. α–β sialon ceramics made from different silicon nitride powders. *J Am Ceram Soc* 1988;**71**:1164–70.
19. Li YW, Wang PL, Chen WW, Cheng YB, Yan DS. Phase formation and microstructural evolution of Ca α-sialon using different Si_3N_4 starting powders. *J Eur Ceram Soc* 2000;**20**:1803–8.
20. Rosenflanz A. α-SiAlON: phase stability, phase transformations, and microstructural evolutions. *PhD thesis*. Michigan University; 1997, p. 178–9.
21. Mandal H, Kara F, Kara A, Turan S. Multication doped alpha-beta SiAlON ceramics. *US Patent, 2004/0067838 A1*.
22. Evans AG, Charles EA. Fracture toughness determinations by indentation. *J Am Ceram Soc* 1976;**59**:371–2.
23. Niihara K, Morena R, Hasselman PH. Evaluation of K_{Ic} of brittle solids by the indentation method with low crack-to-indent ratios. *J Mater Sci Lett* 1982;**1**:13–6.
24. Boris EL, Zhmud V, Bergstrom L. Dissolution and deagglomeration of silicon nitride in aqueous medium. *J Am Ceram Soc* 2000;**83**:2394–400.
25. Sun W-Y, Yan D-S, Gao L, Mandal H, Thompson DP. Subsolidus phase relationships in the systems Ln_2O_3–Si_3N_4–AlN–Al_2O_3 (Ln = Nd, Sm). *J Eur Ceram Soc* 1995;**15**:349–55.
26. Camuscu N, Thompson DP, Mandal H. Effect of starting composition, type of rare earth sintering additive and amount of liquid phase on alpha-beta sialon transformation. *J Eur Ceram Soc* 1997;**17**:599–613.
27. Chatfield C, Ekstrom T, Mikus M. Microstructural investigation of alpha-beta yttrium sialon materials. *J Mater Sci* 1986;**21**:2297–307.
28. Kingery WD. Densification during sintering in the presence of a liquid phase. I. Theory. *J Appl Phys* 1959;**30**:301–6.
29. Cao GZ, Metselaar R. α-Sialon ceramics: a review. *Chem Mater* 1991;**3**:242–52.